

High-resolution helix orientation measured in actin-bound myosin: applications of EPR using a bifunctional spin label

Katie Tuininga, Benjamin P. Binder, & David D. Thomas
Biochemistry, Molecular Biology & Biophysics, University of Minnesota, Minneapolis, MN



Abstract

Myosin II interacts with actin filaments in muscle fibers to generate contractile force in a catalytic cycle involving formation of crossbridges and ATP hydrolysis. Mutations in the heavy chain of myosin have been linked to hypertrophic cardiomyopathy, (HCM) a heritable disease characterized by hypertrophy of the left ventricle and often associated with sudden cardiac death. In this study, we explore the effects of known HCM mutations on the structural dynamics of myosin in the actomyosin complex. Myosin mutant constructs of the catalytic domain were created by site-directed mutagenesis and expressed in *Dictyostelium*. Purified protein was then labelled with a BSL probe, and electron paramagnetic resonance spectroscopy was performed on a muscle fiber decorated with the labelled actomyosin complexes to determine the structural orientation of the myosin mutants relative to the actin fiber axis. Preliminary EPR spectra of actomyosin structural dynamics under different nucleotide-binding conditions provides a platform for quantifying structural perturbations caused by mutations in myosin's catalytic domain.

Background

Functional Role of Myosin and Actin in Muscle Contraction

The motor protein myosin II provides the mechanical force in cardiac and skeletal muscle contraction. The myosin heavy chain exists as a homodimer, with each protomer consisting of three domains: the catalytic domain (CD), light chain domain (LCD), and rod domain. Myosin generates contractile force in muscles by undergoing a series of structural changes coupled to biochemical reactions, in which myosin binds actin filaments present in the myofibrils of muscle fibers and hydrolyzes ATP¹.

This catalytic cycle is characterized by several well-defined steps, with structural changes in myosin influencing its affinity for both actin and nucleotide (Figure 1)^{2,3}. Because the interaction between myosin and actin is integral to crossbridge cycling and subsequent muscle contraction, characterization of myosin in a physiologically-relevant context requires the presence of actin.

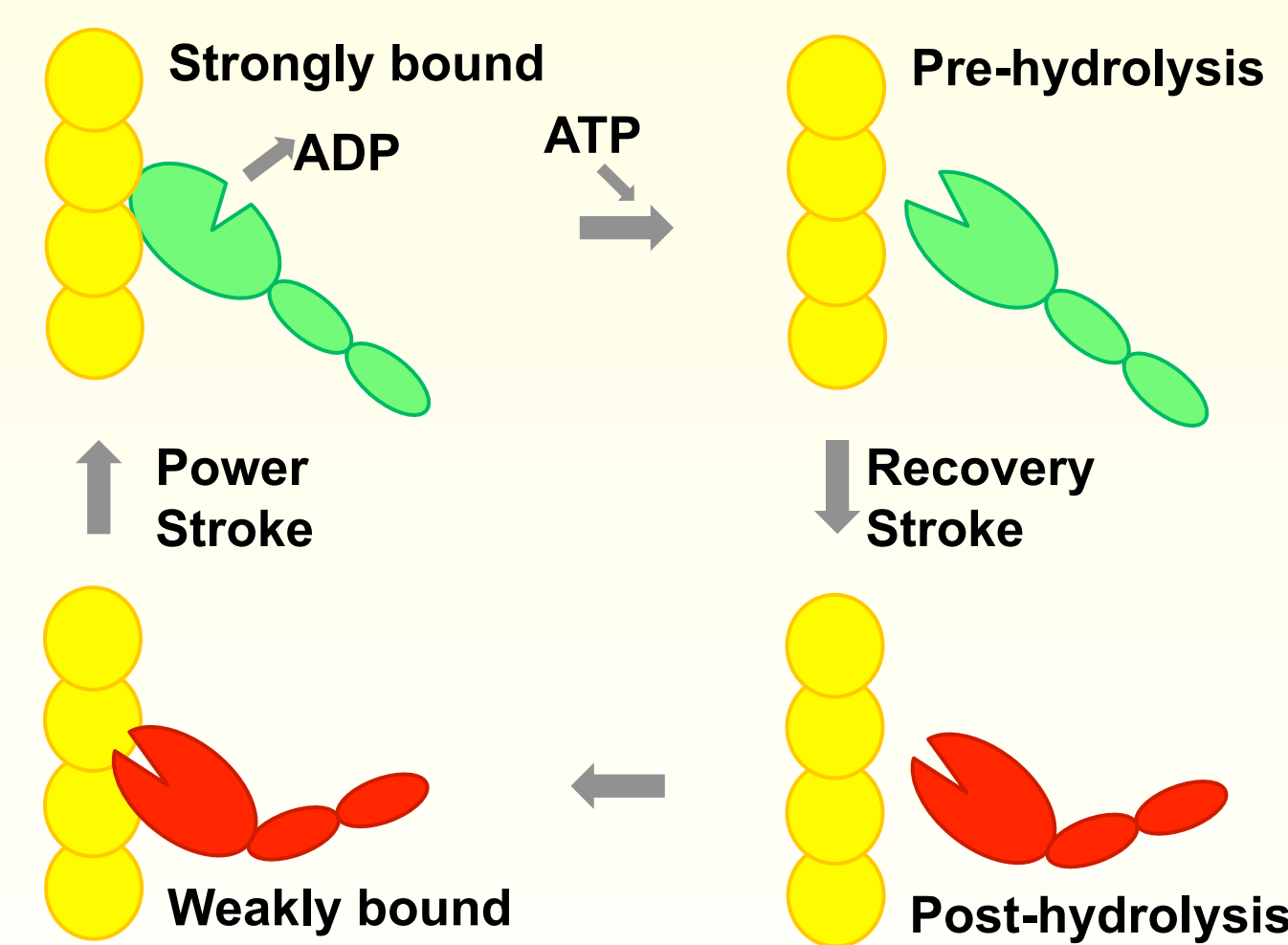


Figure 1. Myosin's catalytic cycle, showing transitions between strong- (green) and weak-binding (red) actin-binding states.

Hypertrophic Cardiomyopathy (HCM) and Myosin Mutations

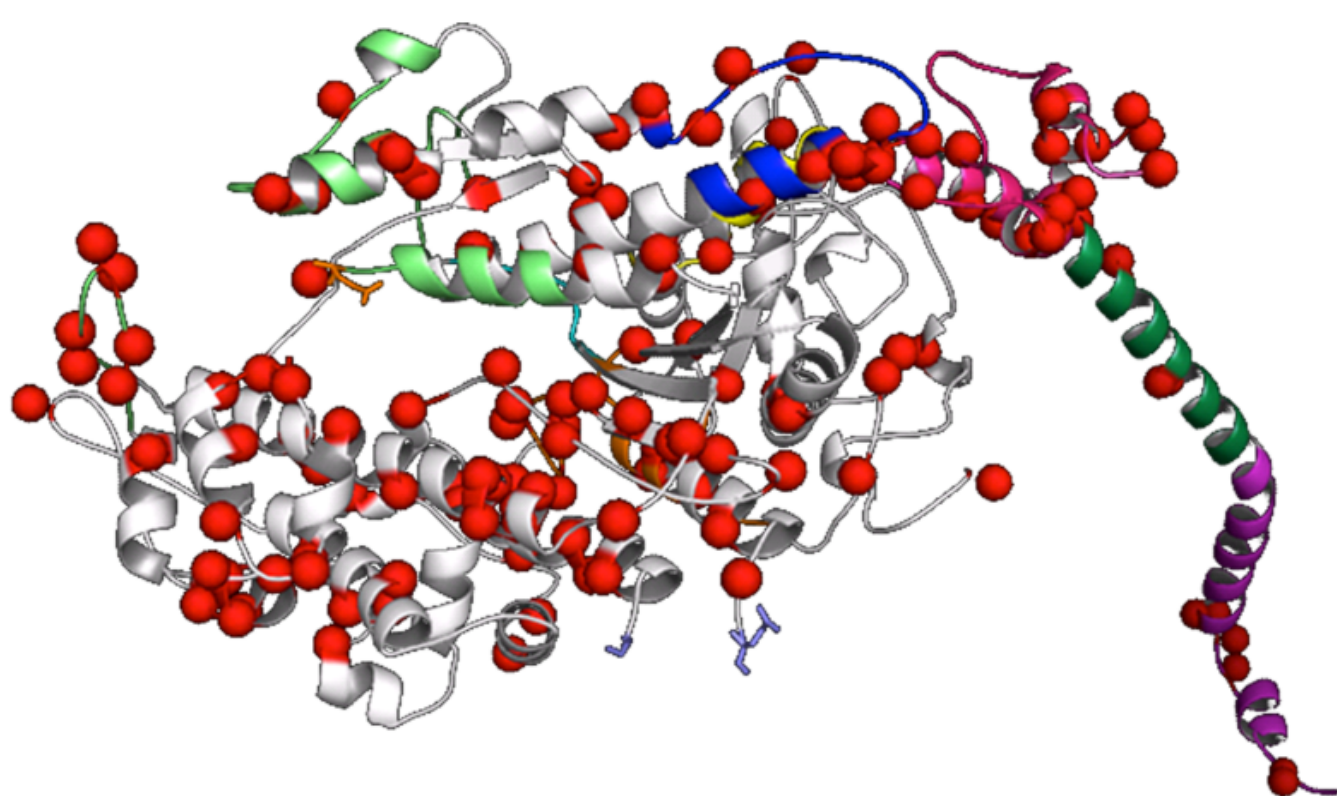


Figure 2. Myosin heavy chain subfragment-1. Residues associated with cardiomyopathy mutations are highlighted in red.

Mutations in the myosin heavy chain have been implicated in hypertrophic cardiomyopathy, a heritable condition associated with sudden cardiac death^{4,5}. Furthermore, myosin mutations are credited as the second greatest leading cause in the development of HCM (Figure 2)⁶. In this study we characterize the functional effects of several mutations in the catalytic domain of myosin on its interaction with actin.

Electron Paramagnetic Resonance (EPR)

Currently no crystal structures of actin and myosin are available, necessitating the use of site-directed techniques to investigate individual structural elements. Because fluorescent probes are relatively insensitive to orientation and are too large for resolving accurate structural constraints, we employ EPR spectroscopy and spin labels as a viable alternative. Most spin labels used in EPR for structural measurements are monofunctional, with characteristic flexibility and nanosecond motion that obscures the orientation dependence of the spectrum. To avoid this, we use a bifunctional spin label (BSL) attached at residue sites $i, i+4$ on a helix, effectively immobilizing the spin label with respect to the protein backbone (Figure 7).

Methods

Myosin Constructs

All constructs were generated using a "Cys-lite" (i.e. all reactive cysteine residues mutated out) *Dictyostelium* Myosin II catalytic domain (S1dC) background. Spin-labeling sites (cysteine residues) were engineered previously at positions 492 and 496 on the C-terminal end of the myosin relay helix (Figure 3).

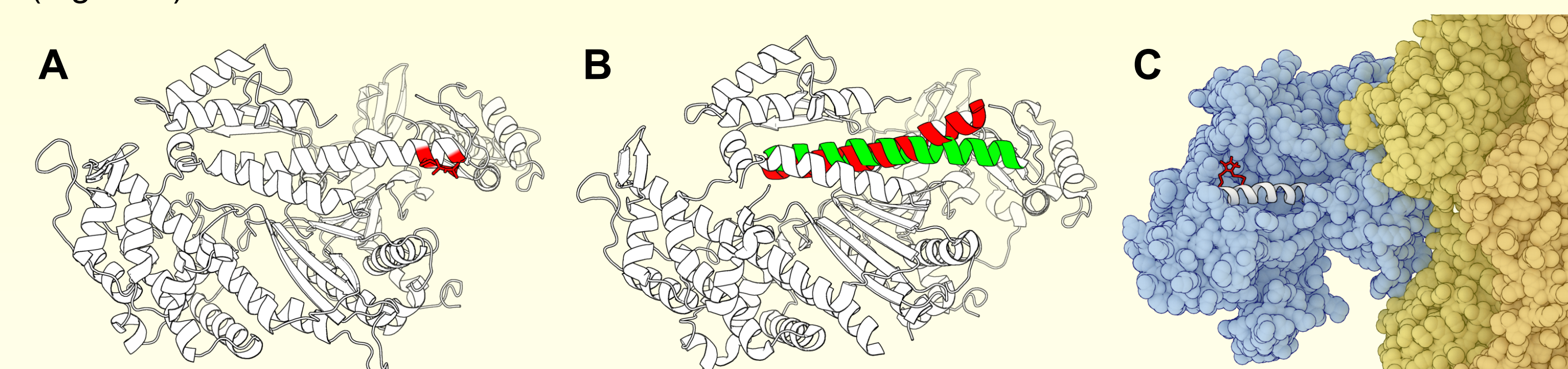


Figure 3. (A) The myosin CD background used for subcloning of all HCM mutations, with BSL modeled on the C-terminal end of the relay helix at positions 492 and 496 (red). (B) Relay helix is of structural interest because of a nucleotide-induced conformational change that mirrors the movement of the motor's lever arm (colors correspond to those in Figure 1). (C) Myosin (blue) bound to actin (yellow) in the rigor state, with relay helix (white) and BSL (red) highlighted.

Site-Directed Mutagenesis

HCM myosin constructs were generated by site-directed mutagenesis using the TOPO vector for amplification in *E. coli*. The presence of each mutation was verified by sequencing, and the myosin insert restricted out of the TOPO vector and ligated into the vector pDXA-3H for expression in the slime mold *Dictyostelium*, which serves as a model study system for human cardiac myosin (Figure 4). After induction of protein expression in Dicty, myosin protein was purified by its expressed N-terminal histidine tag on a cobalt column.

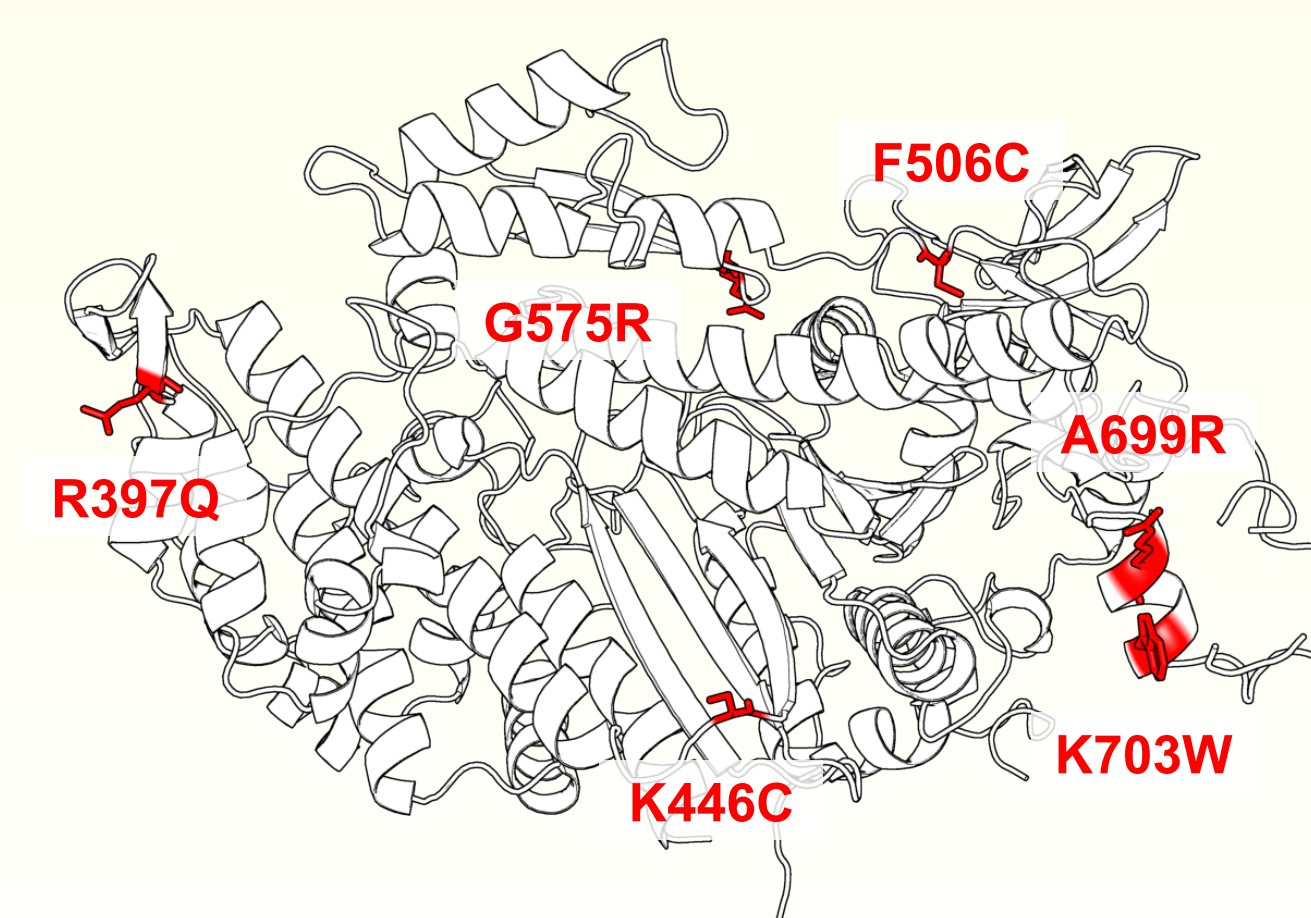


Figure 4. Cardiomyopathy mutants chosen for initial study, highlighted in red.

Electron Paramagnetic Resonance (EPR)

The purified myosin was bifunctionally spin-labelled with a BSL probe at the engineered cysteine residues by dual disulfide linkages. A skinned rabbit psoas fiber was decorated with the labeled myosin, and EPR spectroscopy performed on the oriented muscle fiber (aligned parallel to the applied magnetic field). The principle angles of the nitroxide spin label were then measured relative to the actin filament axis (Figure 5). Initial studies verify that BSL is immobilized and ordered on the relay helix, in the absence of nucleotide (Figure 6).

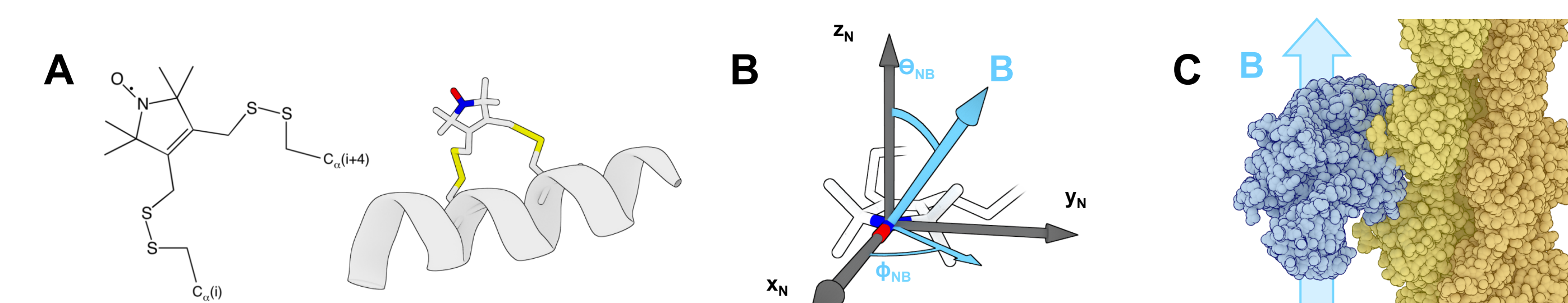
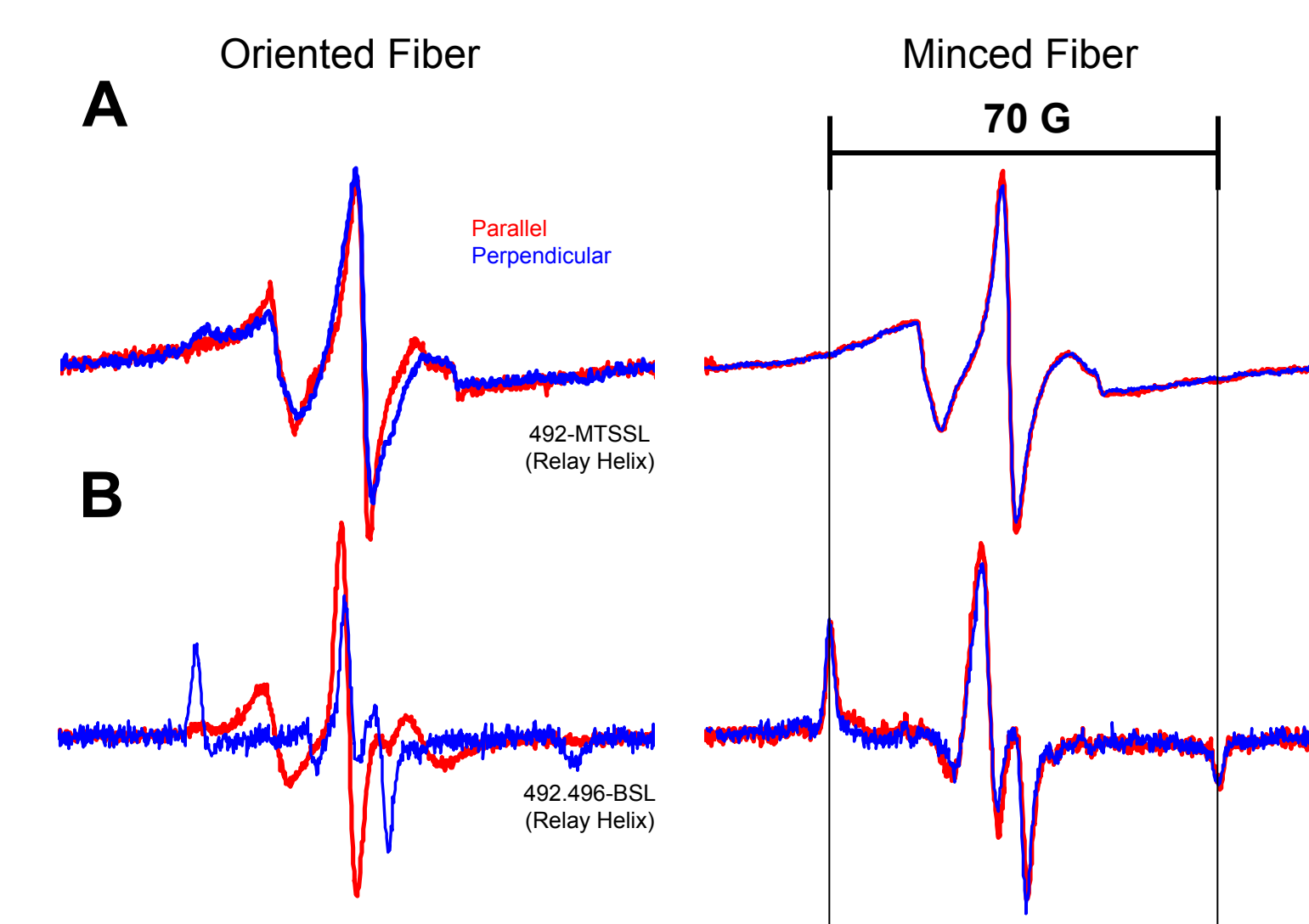


Figure 5. (A) The structure of BSL and its dual disulfide linkage to an α -helix at positions i and $i+4$. (B) Angles θ_{NB} and ϕ_{NB} that define the orientation of the nitroxide spin label (defined by axes x_N, y_N, z_N) relative to the applied magnetic field B , which determine directly the orientation dependence of the EPR spectrum. (C) Orienting the helically ordered muscle fiber (and thus the actin filament axis) with the applied magnetic field B permits direct measurement of the nitroxide orientation relative to actin.

Figure 6. (A) The use of a traditional monofunctional label at an equivalent site on myosin's relay helix demonstrates the problem of nanosecond motion enabled by flexible linkage; fibers oriented parallel and perpendicular to the field (red and blue, left) show no significant orientation dependence, and the spectrum is affected by significant motional narrowing (minced fiber preparations, right). (B) In contrast to (A), the BSL-labeled bifunctional constructs show great disparity between parallel and perpendicular orientations, indicating order (red and blue, left); the minced fiber preparations show no significant nanosecond motion (wide-split, "powder" lineshape on right).



Preliminary Results

We are currently in the process of introducing the HCM mutations into the myosin sequence through site-directed mutagenesis and expressing the mutants in *Dictyostelium*. Preliminary EPR spectra relating functional myosin structural orientations relative to actin at different stages in the catalytic cycle provides a method for comparison to future EPR spectra obtained for mutant myosin (Figure 7)⁷. Thus, this EPR spectra will elucidate different structural perturbations in the actomyosin complex depending upon the location of the point mutation. We hypothesize that the orientation angles of the spin label (and thus myosin) to the actin filaments aligned along the magnetic field will vary considerably depending on the site of the mutation and nucleotide-binding state.

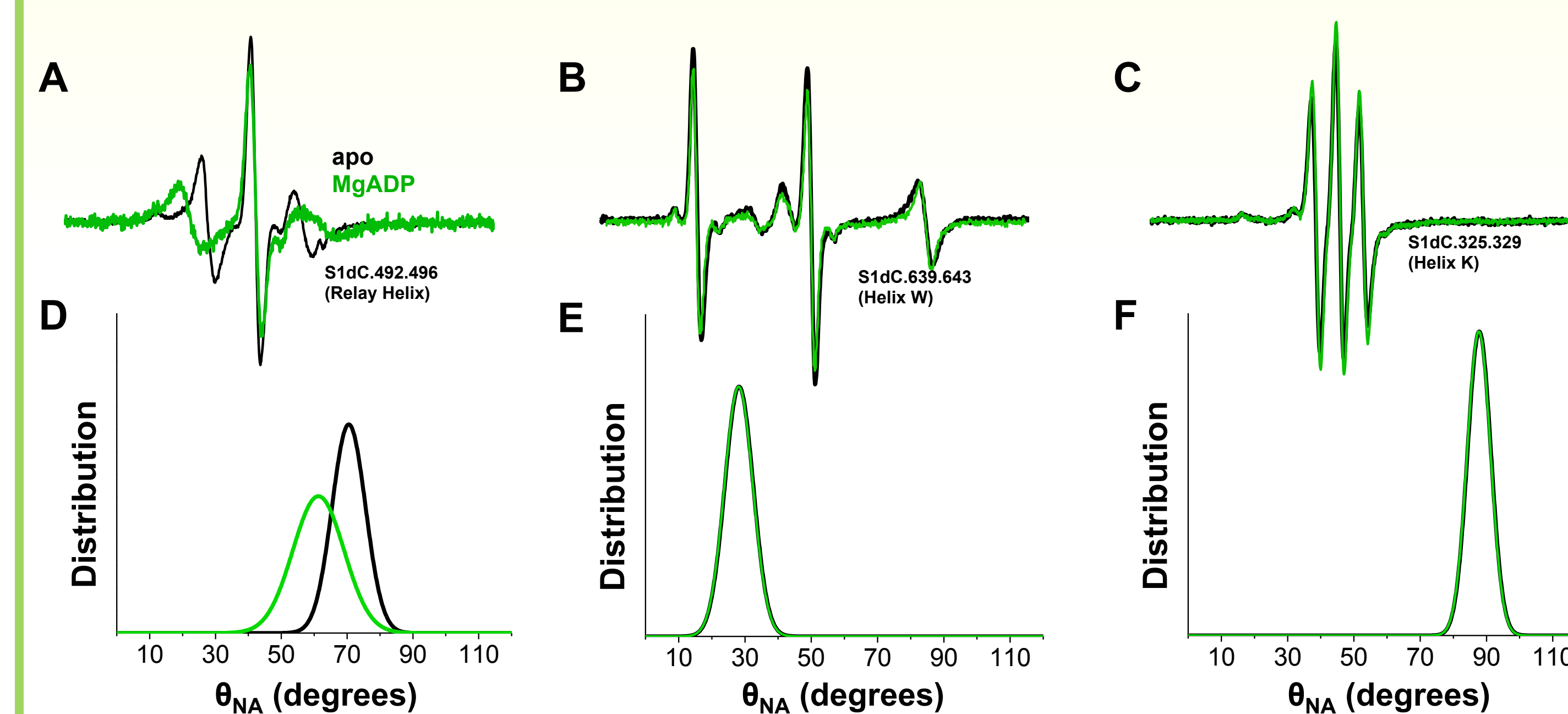


Figure 7. (A-C) EPR spectra from oriented fibers decorated with the 3 labeled myosin constructs, in the absence of nucleotide (black) and the presence of 5mM MgADP (green). (D-F) Angular distributions for the spin label nitroxide principal axis relative to the magnetic field, generated by fitting of simulated spectra to the data.

Conclusions

In order to better understand the impact of mutations associated with hypertrophic cardiomyopathy on myosin structural dynamics, we are utilizing electron paramagnetic resonance as a novel approach to visualizing deviations in myosin's orientation to actin in the actomyosin complex. We predict that mutations occurring in different key regions affect the internal structure of myosin and thus its interactions with actin and nucleotide differently, which will be illustrated in the EPR spectra of the nitroxide spin label orientations relative to the actin fiber axis.

References

- Tyska MJ, Warshaw DM. 2002. The myosin power stroke. *Cell Motility and the Cytoskeleton* 51(1):1-15.
- Preller M, Homes KC. 2013. The myosin start-of-power stroke state and how actin binding drives the power stroke. *Cytoskeleton* 70(10): 651-660.
- Thomas DD, Kast D, Korman VL. 2009. Site-directed spectroscopic probes of actomyosin structural dynamics. *Annual Review of Biophysics* 38: 347-369.
- Fujita H, Sugiura S, Momomura S, Omata M, Sugi H, Sutoh K. 1997. Characterizations of mutant myosins of *Dictyostelium discoideum* equivalent to human familial hypertrophic cardiomyopathy mutants: molecular force level of mutant myosins may have a prognostic implication. *Journal of Clinical Investigation* 99(5): 1010-1015.
- Oldfors A. 2007. Hereditary myosin myopathies. *Neuromuscular Disorders* 17:355-367.
- Maron BJ, Maron MS. 2013. Hypertrophic cardiomyopathy. *Lancet* 381:242-255.
- Binder BP, Cornea S, Thomas DD. 2015 (submitted). High-resolution helix orientation in actin-bound myosin determined with a bifunctional spin label.

Acknowledgements

Sinziana Cornea and Sarah E. Blakely for protein prep and Margaret Titus for facilities and advising in protein preparation (University of MN). EPR was recorded in the Biophysical Spectroscopy Facility (University of MN). Supported by grants from NIH (R01 AR32961, T32 AR07612, P30 AR0507220).

